

# Influence of pressure and temperature on explosion characteristics of COG/air mixtures measured in 20-L and 1000-L spherical vessels

JAN SKŘÍNSKÝ

Energy Research Centre

VŠB-TU Ostrava

17. Listopadu 15/2172, 708 33 Ostrava

CZECH REPUBLIC

jan.skrinsky@vsb.cz <http://vec.vsb.cz/>

*Abstract:* Most explosion characteristics published so far are valid for specific and limited conditions. No explosion characteristic exists for COG which cover all conditions occurring in “real life” and resulting conditions. This requires more information and systematic investigation of the explosion parameters of COG in air under various conditions. Two experimental models were used with the aim at simulating the gas explosion in the middle scale explosion vessels, and the associated effects of the temperature for different gas/air concentrations. The explosion pressures and the rate of pressure rise were determined as a function of the fuel/air ratio at different initial temperatures and pressures. Based on these experimental data, the maximum explosion pressure and the maximum rate of pressure rise were determined as a function of pressure and temperatures. The deflagration index and also the laminar burning velocity were calculated from these data too and compared with the experimental results measured in 20-L and 1000-L spherical vessels.

*Key-Words:* Coke Oven Gas; Combustion and Safety Characteristic data; Maximum Explosion Pressure; Maximum Rate of Pressure Rise; 20-L Explosion Vessel; 1000-L Explosion Vessel

## 1 Introduction

All process industry accidents fall under three broad categories fire, explosion, and toxic release. Of these, fire is the most common, followed by explosions. Within these categories explosion make the immediate damage potential [1]. Coke oven gas (COG) is highly rated as a valuable by-product of coal carbonization to produce coke in the steel industry [2].

Although COG is regarded as a non-standard gaseous fuel, it still has a reasonable energy content and calorific value, which depend on the nature of coal and the type of carbonization and have been widely used together with blast furnace gas and converter gas in the steel industry in Moravian-Silesian region of Czech Republic.

However, coke oven gas is a flammable and explosive substance. Improper operation in the process of production, usage, transportation and storage can easily lead to combustion and explosion, posing a serious threat to lives and property. Therefore, how to safely and effectively utilize or dispose of coke oven gas has become an urgent task [3].

There are no explosion characteristic exists for COG which cover all conditions occurring in “real life” initial conditions. Most explosion

characteristics published so far are valid for specific and limited conditions.

Few data at standard conditions are available in open literature [4]. In the presented paper, these characteristics have been systematically examined and determined in the 20-L and 1000-L explosion chambers for the first time.

## 2 Problem Formulation

Most explosion characteristics published so far are valid for pure compounds and limited experimental conditions, mostly ambient. There have been no explosion characteristic exists for COG-air mixtures which cover industrial conditions up to 423 K and initial pressures 0.50 bar, 0.75 bar and 1.00 bar. The explosion characteristics investigated in this study were explosion pressure,  $P_{ex}$ , maximum explosion pressure,  $P_{max}$ , rate of explosion pressure rise,  $(dp/dt)_{ex}$ , maximum rate of explosion pressure rise,  $(dp/dt)_{max}$ , lower flammable limit, LEL, and upper flammable limit, UEL.

$P_{ex}$  is defined as the highest pressure occurring in a closed vessel during the explosion of a specific mixture of flammable gases with air or air and inert gases determined under specified test conditions.

$P_{\max}$  is defined as the maximum value measured in the tests for explosion pressure when the content of the flammable gas in the mixture is varied.

$(dp/dt)_{\text{ex}}$  is defined as the highest value of the slope (first derivative) of the pressure-time curve (smoothed if necessary), measured in a closed vessel during the explosion of a specific mixture of flammable gases with air or air and inert gases determined under specified test conditions.

$(dp/dt)_{\max}$  is defined as the maximum value of the rate of explosion pressure rise, when varying the content of flammable gas in the mixture.

LEL is defined as the minimum concentration of a combustible substance that is capable of propagating a flame in a homogeneous mixture of the combustible and a gaseous oxidizer under the specified conditions of test.

UEL is defined as the the maximum concentration of a combustible substance that is capable of propagating a flame in a homogeneous mixture of the combustible and a gaseous oxidizer under the specified conditions of test.

The aim of the investigations reported here was to characterize the explosion of COG/air mixtures in closed vessels under different initial conditions of concentration, pressure, and temperature and vessel volume.

### 3 Experiment

#### 2.1 Experimental device

Measurements of the  $P_{\max}$  and  $(dP/dt)_{\max}$  have been performed in the 20-L and 1000-L explosion chambers (OZM Research s.r.o., Czech Republic). Explosion tests have been performed at different initial concentration of COG with the air at standard initial temperature and pressure ( $T_{\text{init}} = 298.15$  K,  $P_{\text{init}} = 1$  bar) and elevated temperature and pressure ( $T_{\text{init}} =$  up to 423 K,  $P_{\text{init}} = 0.5$ -1.0 bar).

The vessel is provided with an opening of an inside diameter of 800 mm, which is provided with a flange and a lock for locking the door closing in the shape of spherical segments. Lock is locking by hydraulic actuator with safety position sensing "locked." Explosion chamber is made of structural steel.

The material and components comply with the use of equipment for experiments at atmospheric initial pressure and initial laboratory temperature (20-25 °C). The system is sealed to the extent that the occurrence of an explosive atmosphere during normal operation outside the delivered system is not

supposed. The chamber is also equipped by the glass window to allow monitoring and high-speed camera experiments of the processes inside the chamber.

Both explosion chambers are equipped with measurement of time depended dynamic pressure using two pressure sensors (Kistler type 701A, accuracy: 0.00125 MPa, sampling rate: 400 ks/s) and by the measurement of the flash duration. For this purpose, it is fitted with a flange having an inner diameter DN 100 and holes for mounting the sensors.

Pressure range is up to 25 MPa calibrated for the range up to 2.5 MPa. Working temperature is up to 200 °C. The entire control of explosion chamber and management of the experiments is concentrated in the main distributor.

The ignition source was mounted such that the electrodes end in the center of the sphere. A series of induction sparks between two electrodes has been used as the ignition source. The electrodes have been positioned at the centre of the vessels. They have pointed rods with a maximum diameter of 4 mm. The angle of the tips have been 60°. The distance between the tips have been  $(5 \pm 0,1)$  mm. A high voltage transformer, with a root mean square of 13 kV to 16 kV and a short circuit current of 20 mA to 30 mA, have been used for producing the ignition spark.

Control of the mechanical parts of the chamber, dispersing system control, ignition system, the system for the preparation of initial internal atmospheres other than air, including homogenization, data acquisition system to record the data have been connected to the main distributor. Control has been ensured through the programming logic controller (PLC) Siemens S7-1200. The signals from the main distributor are transmitted to the auxiliary distributor located directly on the chamber stand. This auxiliary distributor is used to distribute the signals to individual action elements.

The control program contains a procedure enabling the evaluation of the measured data and generating output protocol. Evaluation of pressure curves in terms of the maximum achieved pressure, maximum rate of pressure rise and duration of a flash is done automatically. However, the user is enabled to make reading of these values also manually with a pair of "cursor" and "Zoom" function. The evaluation of a whole series of tests with a single gas has been done for the output protocol and values  $P_{\max}$ ,  $(dp/dt)_{\max}$ , LEL and UEL are recorded together with the concentration at which the maximum values were reached.

The experimental arrangements used in this study are depicted in Fig. 1-2.

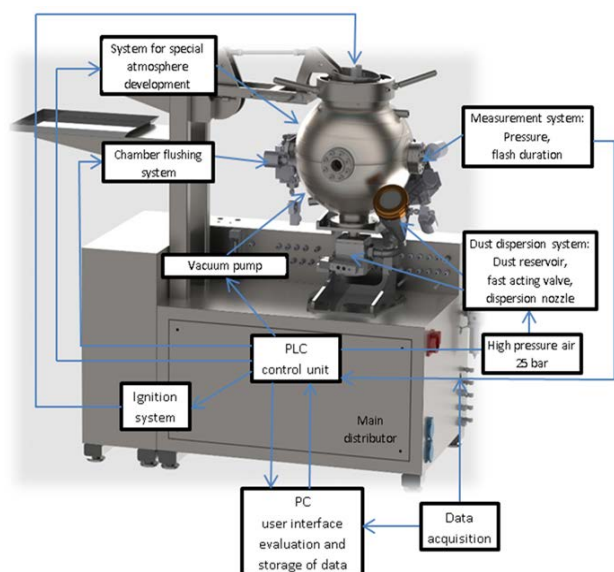


Fig. 1. 20-L vessel experimental arrangement.

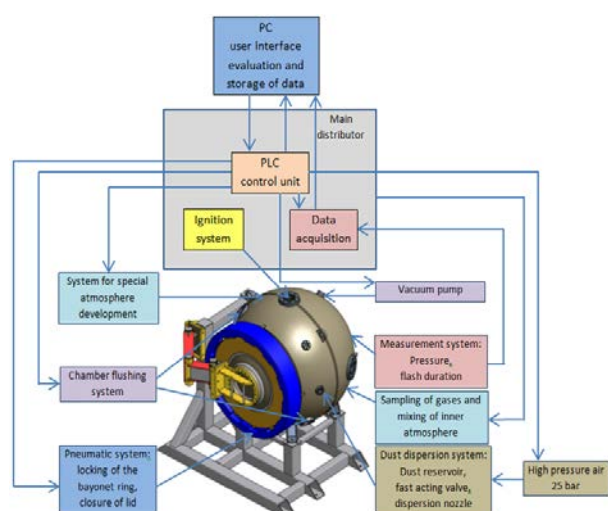


Fig. 2. 1000-L vessel experimental arrangement.

## 2.2 Experimental procedures

The experimental procedure was as follows: (a) the air in the explosion vessel was evacuated to a vacuum of 0.1 mbar; (b) mixing gases were added into the vessel at different ratios; (c) the mixture was admitted at the desired pressure, then ignited at once; (d) after ignition and the capture of the signals by the acquisition system, the burned gas was completely evacuated. Then, a new cycle was repeated [5].

## 2.3 Coke oven gas used in the experiment

The gases used in the experiment included coke oven gas (main components given in Figure 3 and

Table 1), air ( $O_2$  and  $N_2$ ). Relationship between the individual ingredients (in vol.%) concentration in COG produced in Moravian-Silesian region of Czech Republic.

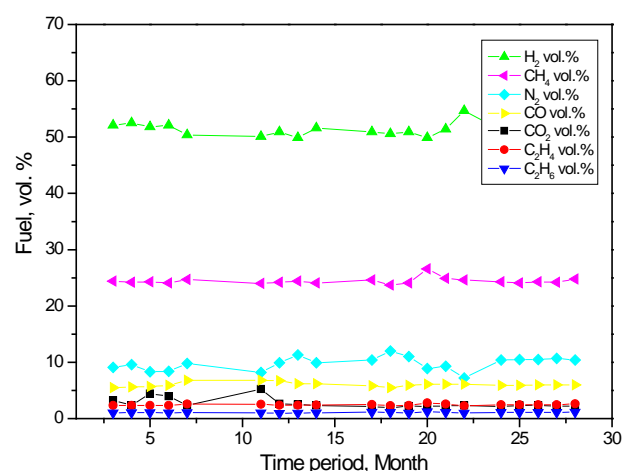


Fig. 3. Compositions of COG for the 20-L experiments.

The compositions of COG for the experiments are taken from the month averages of real coke oven gas concentration from industrial by-product of coal carbonization [10]. The real sample of given composition has been taken into the 50-L Tedlar Gas Sampling Bags and tested in 20-L explosion chamber as received.

Table 1 Compositions of COG for the 1000-L experiments.

Ingredients	Content vol. %
$H_2$	$51.2 \pm 0.5$
$CH_4$	$24.4 \pm 0.3$
CO	$6.0 \pm 0.18$
$C_2H_6$	$1.2 \pm 0.01$
$C_2H_4$	$2.4 \pm 0.02$
$CO_2$	$2.6 \pm 0.02$
$N_2$	$12.2 \pm 0.2$

The composition from Table 1 has been used to prepare the gas mixture sample for 1000-L experiments (Certified composition by Siad s.r.o.). The gas mixture sample have been prepared by gravimetric method. Accredia Lat Centre 55 has calibrated the gases used to calibrate the scales. The reported uncertainties of the ingredients in Table 1 are based on the standard uncertainties multiplied by a coverage factor  $k=2$ , providing the level of confidence of approximately 95 %.

## 2.4 Experimental device validation

The  $\text{CH}_4/\text{O}_2/\text{N}_2$  mixture was obtained by using the partial pressure methodology. After vacuum, the combustion vessel was filled by injecting one mixture component. For validation tests the Siad, s.r.o. gases have been used (purity above 99.9995 vol. % for  $\text{CH}_4$ , purity above 99.995 vol. % for  $\text{O}_2$ , purity above 99.995 vol. % for  $\text{N}_2$ ). The pressure time histories of  $\text{COG}/\text{O}_2/\text{N}_2$  mixture for ten analyzed fuel concentrations measured in 1000-L explosion chamber are shown in Figure 4.

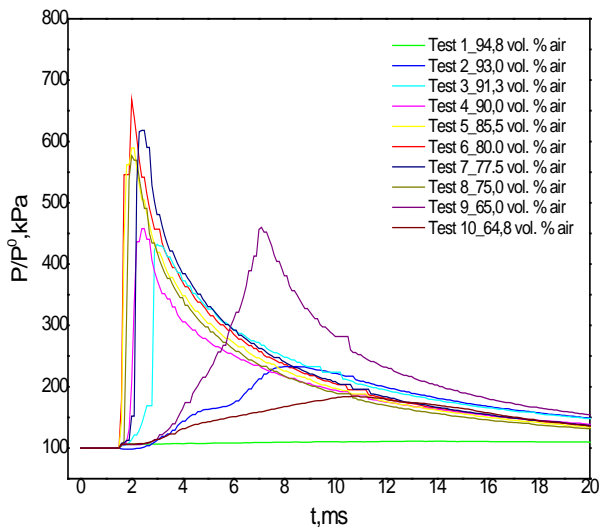


Fig. 4. Relationship between the maximum explosion pressure of COG and its concentration.

Based on the pressure time dependency three regimes of explosion development or combustion conversion can be identified.

In the first one, the pressure increases fast and smoothly to the maximum value, after ignition. This type of pressure development is seen for near-stoichiometric mixtures [6].

In the second regime, the pressure development is present in a narrow fuel lean concentration range and in a wider concentration range with fuel rich mixtures [6].

In the third regime, the increases are low and slow [6].

The adiabatic condition, which certainly at longer explosion time, provides a limitation. Longer explosion times, especially in the second combustion regime, enhance the heat losses in particular at the top of the vessel due to convection and conduction, additionally to radiation.

Calculations of the explosion pressures for methane-air mixtures were done by program GASEQ 0.79 at atmospheric initial conditions.

Fig. 5 illustrates the comparison among peak explosion pressure ( $P_{\text{max}}$ ) and computed „ideal“ adiabatic explosion pressure ( $P_{\text{admax}}$ ) versus fuel fraction at initial atmospheric pressure and temperature.

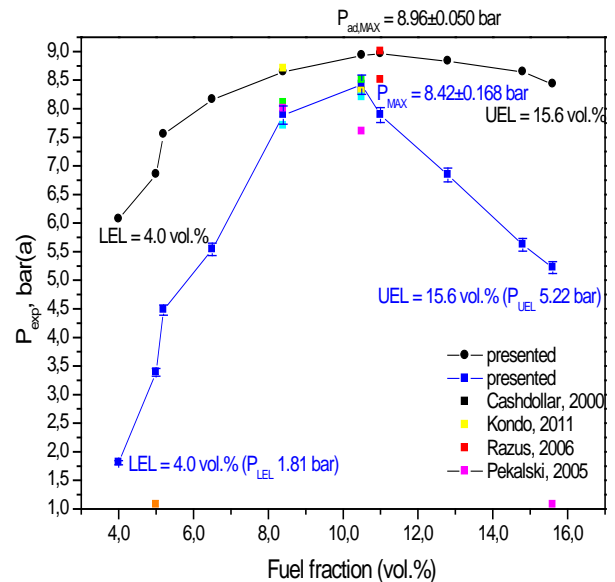


Fig. 5. Calibration for gas mixtures explosions.

Calculated explosion pressures,  $P_{\text{ad}}$ , predictions show a reasonable agreement at the near stoichiometric concentrations. Outside this range the agreement becomes poor, the deviations from the measured values increase when the flammability limits are approached [6].

Fig. 6 illustrates the real non-adiabatic explosion. The red and orange spots in the Fig. 6 illustrates the soot that have been produced during the first phase (i.e. in the first 2 ms) of the explosion.

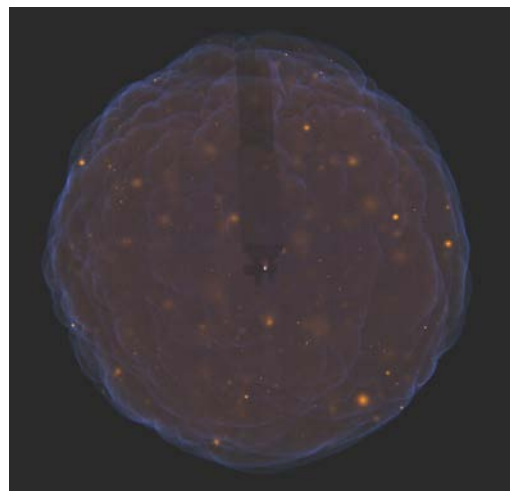


Fig. 6.  $\text{CH}_4/\text{O}_2/\text{N}_2$  spherical flame at  $P_{\text{max}}$ .

Cashdollar et al. [7] reports different values of maximum explosion pressures for methane-air mixtures, depending on the volume of the explosion vessel: 8.30 bar(a) in a  $20.0 \cdot 10^{-3} \text{ m}^3$  explosion vessel and 8.5 bar(a) in a  $120.0 \cdot 10^{-3} \text{ m}^3$  explosion vessel.

The maximum rate of pressure rise  $(dp/dt)_{\max}$  is often employed for explosion characteristics evaluation and used in deflagration index determination. In this previous study, the values of  $(dp/dt)_{\max}$  is for the 120-L and 20-L chambers  $66.0 \pm 2.0 \text{ bar/s}$  and  $92.0 \pm 3.0 \text{ bar/s}$ , respectively, while the LEL was 5.0% for both chambers. There are several studies on flammable limits of  $\text{CH}_4/\text{O}_2/\text{N}_2$  (in vol. %) for flame propagation in quiescent mixtures, with spark ignition.

Further, [8] have reported  $120.0 \cdot 10^{-3} \text{ m}^3$  data on the LEL which show a gradual increase in pressure from 4.9 to 5.0%. The corresponding UEL is 15.0-15.9% based on the newer data. The 12-L glass sphere gave an LEL of  $4.95 \pm 0.1\%$  and UEL of  $15.7 \pm 0.1\%$  [9].

$P_{\max}$  varies from 8.30 bar(a) in a  $20.0 \cdot 10^{-3} \text{ m}^3$  explosion vessel to 8.5 bar(a) in a  $120.0 \cdot 10^{-3} \text{ m}^3$  explosion vessel. LEL varies from 4.9% to 5.0% and UEL from 15.7% to 15.8%.

In conclusion, measured data  $p_{\max} = 8.96 \pm 0.050 \text{ bar(a)}$ ,  $\text{LEL} = 4.0 \text{ vol.}\%$  and  $\text{UEL} = 15.6 \text{ vol.}\%$  were successfully compared with the available published experimental results [7-9].

### 3 Calculation

The maximum explosion pressure in a constant volume chamber can be simulated based on the adiabatic assumption through thermal equilibrium. Such calculations were used for the initial predictions for experiments.

Real explosion is not under the absolute adiabatic condition. It accompanies both radiant and convective heat losses to the wall, leading to the lower  $P_{\max}$  than  $P_{\text{admax}}$ . It is noted that the difference between  $P_{\max}$  and  $P_{\text{admax}}$  is remarkably increased at highly rich mixtures. This is because soot, C(s), formed at rich mixtures due to the absence of oxygen, highly promoting the heat loss through the continuum radiation to the vessel wall [6].

Calculation procedure is described in [3]. Due to the complexity of the involved physical phenomena and to the lack of an adequate amount of reliable experimental data, a number of different models and calculation procedures for estimating the physical consequences following the physical

explosion of a gaseous state are presently reported in the literature.

Two computational approaches have been used for explosion pressure,  $P_{\text{ad}}$ , calculations in this study.

The element potential approach in the thermochemical equilibrium calculations applied in the Chemkin 3.6.2 subroutine using the species and their thermodynamic values from the GRI 3.0 and Konnov 5.0 and the combustion equilibrium calculations by program GASEQ 0.79 obtained from the properties of the reactant species and of equilibrated adiabatic products using the species and their thermodynamic values from the Burcat.thr.

Both chemical equilibrium models assumes adiabatic conditions in constant volume, and formation of equilibrium-defined concentrations of post explosion compounds and their expansion due to the temperature rise caused by the liberated heat assuming ideal gas behavior.

This approach represents ideal deflagrations in closed systems well and gives the highest possible attainable explosion pressures. It has been shown that the model is able to predict, with a reasonable accuracy, the experimental values of the explosion pressures and constant volume adiabatic explosion temperatures in different fuel-enriched conditions, for different types of gaseous explosions [10-11].

The maximum pressure rise rate during gas explosions in enclosures,  $(dP/dt)_{\max}$ , and the deflagration index,  $K_G$ , are important explosion characteristics of pre-mixture. They are used to quantify the potential severity of an explosion.

The maximum pressure rise rate,  $(dP/dt)_{\max}$ , depends not only on the mixture properties (such as mixture composition, initial temperature and initial pressure) but also on the volume of the vessel in which gas explosion takes place. Unlike  $(dP/dt)_{\max}$ , the deflagration index is an intrinsic property of the pre-mixture and it is independent of the volume of the vessel used in experimental measurements.

The relationship between  $K_G$  and  $(dP/dt)_{\max}$  is given by Eq(1):

$$K_G = (dP/dt)_{\max} V^{1/3} \quad (1)$$

in which  $K_G$  is the deflagration index (bar.m/s),  $V$  is the vessel volume ( $\text{m}^3$ ),  $dP/dt$  is the maximum rate of pressure rise (bar/s). In order to capture the intrinsic reactivity of COG mixture, the burning velocity has been obtained from time pressure records of explosions occurring in 20-L closed explosion chamber.

The burning velocity in Eq(3) first published by [6] has been calculated from the pressure time

history by using the time derivative of flame radius,  $r_f$ , as given by the correlation in Eq(2):

$$r_f = (3V/4\pi)^{1/3} [1 - (P_0/P)^{1/\gamma} ((P_{max}-P)/(P_{max}-P_0))]^{1/3} \quad (2)$$

in which  $r_f$  is the flame radius (m),  $V$  is the vessel volume ( $m^3$ ),  $P_0$  is the initial pressure (bar),  $P$  is the actual pressure (bar),  $P_{max}$  is the maximum explosion pressure (bar) and  $\gamma$  the adiabatic coefficient of the unburned gas (-).

$$s = [1 / ((P_{max}-P_0))^{1/3} (4\pi/3V)^{-1/3} (P/P_0)^{1/\gamma} [1 - (P/P_0)^{1/\gamma} ((P_{max}-P)/(P_{max}-P_0))]^{-2/3} dP/dt \quad (3)$$

in which  $s$  is burning velocity (m/s),  $r_f$  is the flame radius (m),  $R$  is specific gas constant (J/kg.K),  $V$  is the vessel volume ( $m^3$ ),  $P_0$  is the initial pressure (bar),  $P$  is the actual pressure (bar),  $P_{max}$  is the maximum explosion pressure (bar),  $\gamma$  the adiabatic coefficient of the unburned gas (-) and  $dP/dt$  is the rate of pressure rise (bar/s).

#### 4 Results and discussion

For all of the mixture compositions investigated (3 tests/5 tests) the mean is given as a result or used in further evaluations.

The increases the flammability range. The upper explosion limit increases and the lower decreases.

Fig. 7,9 illustrate the measured LEL and UEL of the COG/air mixtures. When the COG/air mixture composition approaches, the flammability limits the explosion pressure drops sharply to zero.

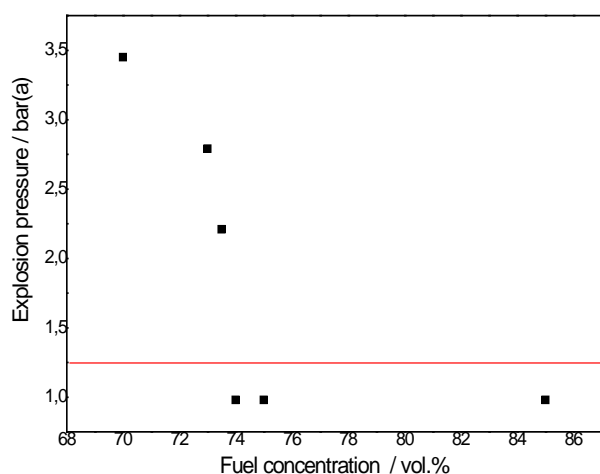


Fig. 7 illustrates the measured LEL of the COG/air mixtures.



Fig. 8 illustrates the measured LEL of the COG/air mixtures.

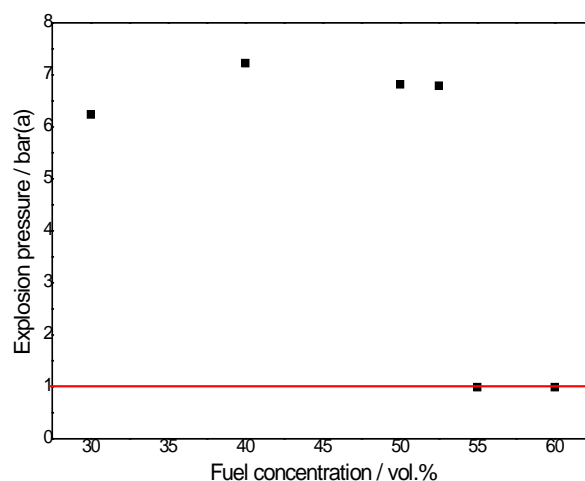


Fig. 9 illustrates the measured UEL of the COG/air mixtures.



Fig. 10 illustrates the measured UEL of the COG/air mixtures.

Table 1 reports the mixture compositions investigated in the second part of this study, together with the corresponding values of adiabatic pressure ( $P_{ad}$ ) at constant volume, as computed by the chemical equilibrium assumption.

The value of equivalence ratio corresponding to fuel-rich mixtures ( $\Phi=1.25-2.25$  i.e.  $C=22.5-32.2$  vol.% of fuel in 77.5-64.8 vol. % of air) has been considered because it corresponds to the maximum value for the laminar burning velocity.

An experimental study on the combustion characteristics of COG/air mixtures was conducted in a constant volume combustion vessel over a wide range of equivalence ratios.

Table 1 Explosion parameters for atmospheric conditions.

$P_{max}$	$8.19 \pm 0.163$ bar(a)
$P_{ad}$	8.58 bar(a)
$T_{pmax}$	1.50 ms
$(dP/dT)_{max}$	$180.12 \pm 18.012$ (bar/s)
$s_l$	1.11 m/s
LEL	5.6 vol. %
UEL	35.2 vol. %

The measured explosion pressures  $p_{ex}$  of COG/air mixtures at various initial temperatures and at various initial pressures are represented versus the equivalence ratio in Fig. 3-4 (mean values from 20-L spherical vessel and 1000-L spherical vessel) at 298-423 K as an example.

For explosion pressure,  $P_{ex}$ , the evaluation of the test is based on the highest pressure of 5 tests carried out with the actual test mixture. In order to take into account all uncertainties (pressure measuring, flammable gas content, calibration, procedure with limited number of tests) this value is rounded up to the nearest 0,1 bar.

For maximum explosion pressure,  $P_{max}$ , the evaluation of the test is based on that test mixture which gives the highest explosion pressure of all.

In Fig. 11, the maximum explosion pressure  $p_{max}$  is found at the equivalence ratio range  $\Phi=0.25-2.18$ , independently of the initial pressure. For all conditions investigated, the experimental explosion pressures show plateaus close to the upper explosion limits.

The normalized maximum explosion pressure is 8.2, 7.7, 6.3 and 5.6 bar(a) at 298 K, 323 K, 373 K, and 423 K at 1.00 bar(a), respectively. Similarly, the normalized maximum explosion pressure is 8.2, 6.1, and 4.1 bar(a) at 1.00 bar(a), 0.75 bar (s), and 0.05 bar(a) at 298 K, respectively.

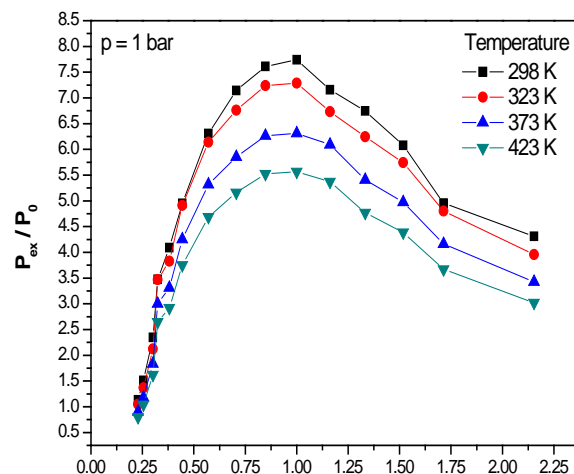


Fig. 12. Normalized peak explosion pressure ( $P_{max}/P_0$ ) versus equivalence ratio at atmospheric pressure and four initial temperatures.

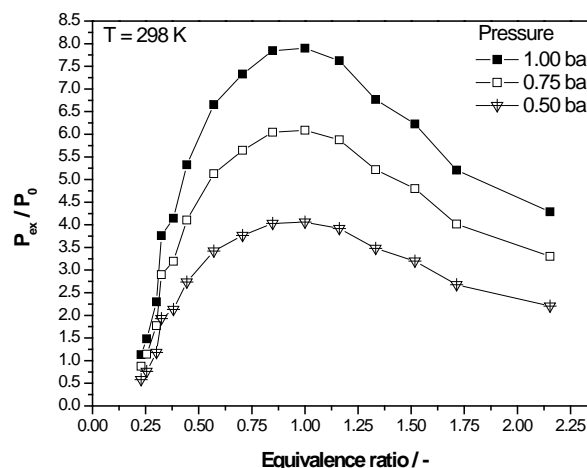


Fig. 13. Normalized peak explosion pressure ( $P_{max}/P_0$ ) versus equivalence ratio at atmospheric temperature and three initial pressures.

As observed from Fig. 12-13 the experimental results, explosion pressure shows a certain regularity with the variation of COG concentration, and the maximum pressure achieves its peak value near the stoichiometric concentration (The calculated value based on the compositions of coke oven gas is 20.9%) and tends to decrease if the concentration is lower or higher than 20.9%.

This pattern forms because near the stoichiometric concentration, the COG and oxygen can be fully utilised, causing the most intense reaction to occur, and thus, the largest pressure value is generated.

When the concentration of COG is less than the stoichiometric concentration, even though there is surplus oxygen, the coke oven gas is also in

relatively shorter supply, so the explosion is relatively weaker, correspondingly producing relatively less pressure.

When concentration of COG is more than the stoichiometric concentration, the oxygen concentration will be relatively low. Thus, the coke oven gas concentration actually involved in the reaction is lower, so less pressure is produced.

The greater the concentration of coke oven gas, the less oxygen content, and therefore the less of the coke oven gas actually participates in the reaction. Thus, the pressure becomes smaller.

For rate of explosion pressure rise,  $(dp/dt)_{ex}$ , the evaluation of the test is based on the highest rate of pressure rise of 5 tests carried out with the actual test mixture. For maximum rate of explosion pressure rise,  $(dp/dt)_{max}$ , the evaluation of the test is based on that test mixture which gives the highest rate of pressure rise. In order to take into account all uncertainties (pressure measuring, flammable gas content, calibration, smoothing), the highest value is rounded up. Rate of pressure rises at the initial temperatures of 298 K, 323 K, 373 K, and 423 K bar(a) are presented in Figure 14.

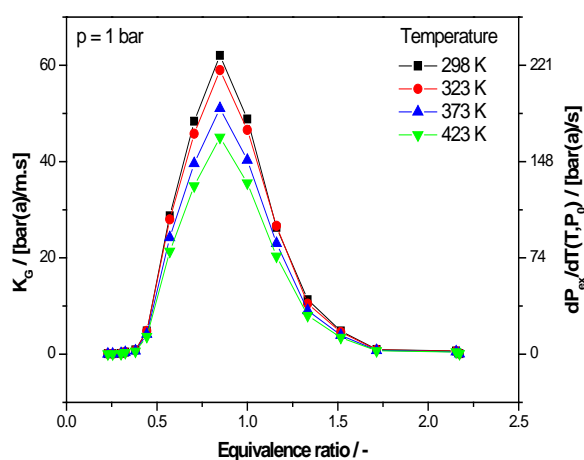


Fig. 14. Rate of pressure rise,  $(dp/dt)_{ex}$ , and deflagration index,  $K_G$ , versus equivalence ratio at elevated temperatures and pressures.

Fig. 14 shows the comparison among rate of pressure rise,  $(dp/dt)_{ex}$ , and deflagration index,  $K_G$ , versus equivalence ratio at elevated temperatures and pressures for the COG/air mixtures.

The maximum rate of pressure rise is 61.9, 58.7, 50.8 and 44.8 bar(a)/m.s at 298 K, 323 K, 373 K, and 423 K at 1.00 bar(a), respectively.

Maximum rate of pressure rise and deflagration index reach their peaks at  $\Phi$  around 1.46, and they decrease at both lean and rich mixtures.

As shown in Fig. 14,  $(dp/dt)_{max}$  and  $K_G$  give an approximate value at varied initial temperatures, indicating that  $(dp/dt)_{max}$  and  $K_G$  are sensitive to the variation of temperature (109, 102, 98, 90 bar(a)/m.s). Rate of pressure rise is affected by both flame speed and heat release. Flame speed increases monotonically with the increase of temperature, but the decrease of total fuel mass results in the decreased heat release and offsets the effect of flame speed on the explosion pressure.

With the increase of initial pressure  $(dp/dt)_{max}$  and  $K_G$  increase dramatically, especially around equivalence ratio of 1.1. This differs from the flame speed, but agrees with the mass burning flux when taking into account of the effect of density. It is noted that deflagration index is less than  $70 \text{ bar}\cdot\text{m}\cdot\text{s}^{-1}$  at  $\Phi=1.0$  and the initial pressure of 1.0 bar, belonging to the first class of deflagration index and low potential of explosion hazard!

However,  $K_G$  could exceed 300 bar(a)/m.s<sup>-1</sup> around the stoichiometric ratio at the pressures higher than 1.0 bar and could enter the highest class of deflagration index. Rate of pressure rises at the initial pressures of 1.00 bar(a), 0.75 bar(a), and 0.50 bar(a) are presented in Figure 15.

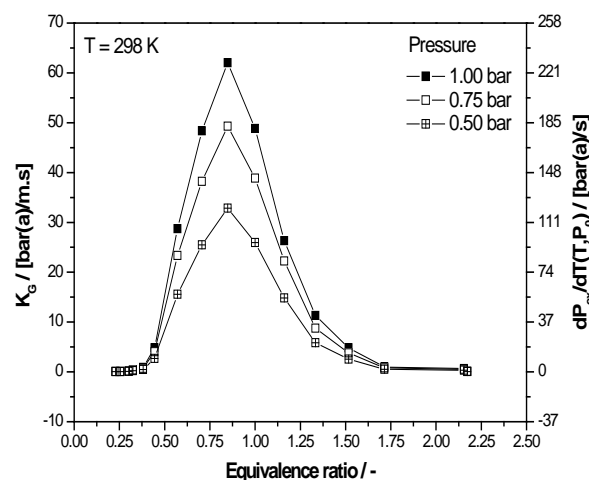


Fig. 15. Rate of pressure rise,  $(dp/dt)_{ex}$ , and deflagration index,  $K_G$ , versus equivalence ratio at elevated temperatures and pressures.

The maximum rate of pressure rise and the maximum explosion pressure have similar relationships with COG concentration (as plotted in Fig. 15).

The maximum rate of pressure rise is 61.9, 49.4, and 32.4 bar(a)/m.s at 1.00 bar(a), 0.75 bar(a), and 0.50 bar(a) at 298 K, respectively.

When the concentration of coke oven gas is lower than its stoichiometric concentration, oxygen is relatively abundant. With the increase of coke oven



gas concentration, its reaction volume per unit time increases, so the maximum rate of pressure rise also increases, and it achieves the maximum value near the stoichiometric concentration ( $\Phi=0.9$ ). However, when the COG concentration is higher than the stoichiometric concentration, increasing the COG concentration requires the oxygen content in the mixture to decline, so the amount of coke oven gas actually involved in the reaction is reduced correspondingly.

Fig. 16 shows by-products mole fractions for Different Equivalence Ratios (heat loss through radiation). As seen in figure the mole fractions of  $\text{CO}_2$  and  $\text{H}_2\text{O}$  all decrease in the order of 298, 323, 373, 423, indicating the heat loss through radiation decreases in the same order. I.

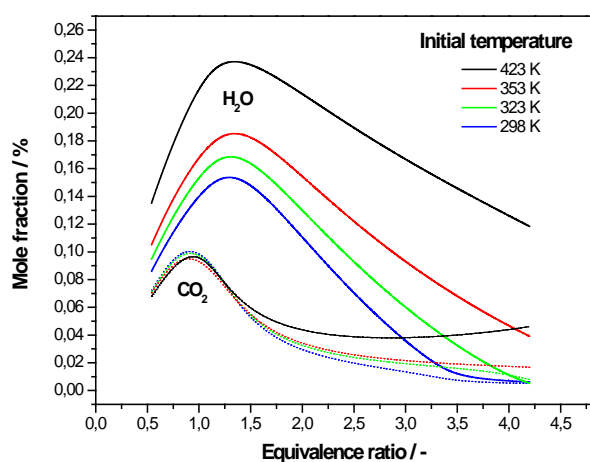


Fig. 16. By-products Mole Fractions for Different Equivalence Ratios (heat loss through radiation).

It is noted that COG experiments present approximate values of  $P_{\max}/P_0$  and  $P_{\text{ad}}/P_0$  at lean mixtures.

However, the difference among the COG flame is much significant for  $P_{\max}/P_0$  than for  $P_{\text{ad}}/P_0$  at the rich mixtures, revealing the most heat is lost in lean mixture flame.

To illustrate this phenomenon, the mole fractions of the main products,  $\text{CO}_2$  and  $\text{H}_2\text{O}$ , in the rich flames are given in figure. Though CO is also important product in the rich fuel flames, it couldn't radiate heat and is not discussed here. As seen in figure, the mole fractions of  $\text{CO}_2$  and  $\text{H}_2\text{O}$  all decrease in the order of 298 K, 323 K, 353 K and 423 K, indicating the heat loss through radiation decreases in the same order.

## 5 Conclusion

An experimental study on the characteristics of COG-air explosions in a 20-L and 1000-L closed spherical vessels with central ignition was carried

out, using COG-air mixtures with variable composition, at various initial temperatures and pressures.

With the increase of initial temperature, the explosion pressure, the maximum rate of pressure rise and the deflagration index were decreased, and a shorter combustion duration and higher normalized mass burning rate were presented.

With the increase of initial pressure, the explosion pressure, the maximum rate of pressure rise and the deflagration index increase, a shorter combustion duration and higher normalized mass burning rate were presented. The more detail findings are summarized as follows:

1. Different explosion characteristics have been reported in a range from 298 K up to 423 K and from 0.5 bar(a) up to 1.0 bar(a).
2. The explosion pressures of COG-air mixtures attained their highest value at a concentration 1.0 within the studied concentration range of 0.25-2.25.
3. Most reliable ("worse case") explosion pressure for constant initial pressure 1.00 bar(a) is the  $p_{\max}$ : 8.2 bar(a) for 298 K, 7.7 bar(a) for 323 K, 6.3 bar(a) for 353 K and 5.6 bar(a) for 423 K.
4. Most reliable ("worse case") explosion pressure for constant initial temperature 298 K is the  $p_{\max}$ : 8.2 bar(a) for 1.00 bar(a), 6.1 bar(a) for 0.75 bar(a), 4.1 bar(a) for 0.05 bar(a).
5. The explosion pressure, the maximum rate of pressure rise, the deflagration index are decreased, while the normalized mass burning rate is increased with the increase of initial temperature.
6. The increase of initial temperature, the peak explosion pressure, combustion duration and flame development period all linearly decrease, while the maximum rate of pressure rise varies little.

This work would not have been possible without the financial support of Innovation for Efficiency and Environment - Growth, reg. no. LO1403 supported by National Programme for Sustainability and financed by the Ministry of Education, Youth and Sports.

### References:

- [1] M. Skřínková et al., BLEVE: Cases, Causes, Consequences and Prevention. *Mat. Sci. For.*, Vol. 811, 2014, pp. 91-94.
- [2] R. Razzaq, Ch. Li, S. Zhang, Coke oven gas: availability, properties, purification, and utilization in China, *China Fuel*, Vol. 113, 2013, pp. 287-299.

- [3] J. Skřínský et al., Explosion characteristics of methane for CFD modeling and simulation of turbulent gas flow behavior during explosion, *AIP Conference Proceedings*, Vol. 1745, 2016, pp. 020057-1-020057-6.
- [4] Z. Zhang, et al., Coke oven gas explosion suppression, *Safety Science*, Vol. 55, 2013, pp. 81-87.
- [5] EN 15967, 2012. Determination of maximum explosion pressure and the maximum rate of pressure rise of gases and vapours. European Standard, Beuth Verlag, Berlin Wien Zurich.
- [6] A. A. Pekalski et al. Determination of the Explosion Behaviour of Methane and Propene in Air or Oxygen at Standard and Elevated Conditions, *Process Safety and Environmental protection*, Vol. 83, No. B5, 2005, pp. 421-429.
- [7] K. L. Cashdollar et al. Flammability of methane, propane, and hydrogen gases. *Journal of Loss Prevention in the Process Industries*, Vol. 13, No. 3-5, 2000, pp. 327-340.
- [8] S. Kondo et al., On the temperature dependence of flammability limits of gases, *J. Hazard Mater*, Vol. 187, No. 1, 2011, pp. 585-590.
- [9] D. Razus, D. Oancea, C. Movileanu, Burning velocity evaluation from pressure evolution during the early stage of closed-vessel explosion, *Journal of Loss Prevention in the Process Industries*, Vol. 19, No. 4, 2006, pp. 334-342.
- [10] J. Skřínský et al., Explosion parameters of Coke oven gas in 1 m<sup>3</sup> explosion chamber, *Chemical Engineering Transactions*, Vol. 53, 2016, pp. 7-12.
- [11] M. Skřínková et al. Mathematical models for the prediction of heat flux from fire-balls. *WSEAS Transactions on Heat and Mass Transfer*, Vol. 9, No. 1, 2014, pp. 243-250.